ORIGINAL ARTICLE

Lapachol and (α/β)-Lapachone as Inhibitors of SARS-CoV-2 Main Protease (Mpro) and hACE-2: ADME Properties, Docking and Dynamic Simulation Approaches

Mejdi Snoussi[1,2], Iqrar Ahmad[3], Harun Patel[3], Emira Noumi[1,4], Rafat Zrieq[5], Mohd Saeed[1], Shadi Sulaiman[6], Nasrin E. Khalifa[7,8], Fakher Chabchoub[9], Vincenzo De Feo[10], Mohamed A. M. Gad-Elkareem[11], Kaïss Aouadi[12,13], Adel Kadri[14,15]

[1]Department of Biology, University of Hail, College of Science, P.O. Box 2440, Ha'il 2440, Saudi Arabia, [2]Laboratory of Genetics, Biodiversity and Valorisation of Bioressources, High Institute of Biotechnology--University of Monastir, Monastir 5000, Tunisia, [3]Division of Computer Aided Drug Design, Department of Pharmaceutical Chemistry, R. C. Patel Institute of Pharmaceutical Education and Research, Shirpur, Maharashtra 425405, India, [4]Laboratory of Bioressources: Integrative Biology and Recovery, High Institute of Biotechnology--University of Monastir, Monastir 5000, Tunisia, [5]Department of Public Health, College of Public Health and Health Informatics, [6]Department of Clinical Laboratory Sciences, Faculty of Applied Medical Sciences, University of Ha'il, Ha'il, [7]Department of Pharmaceutics, College of pharmacy, University of Hail, Kingdom of Saudi Arabia, [8]Department of Pharmaceutics, Faculty of Pharmacy, University of Khartoum, Sudan, [9]Laboratoire de Chimie Appliquée: Hétérocycles, Corps Gras et Polymères, Faculté des Sciences de Sfax, Université de Sfax. B. P, 802. 3000 Sfax, Tunisie, [10]Department of Pharmacy, University of Salerno, Via Giovanni Paolo II, 132, Fisciano, Salerno 84084, Italy, [11]Department of Chemistry, Faculty of Science, Al--Azhar University, Assiut 71524, Egypt, [12]Department of Chemistry, College of Science, Qassim University, Buraidah 51452, Saudi Arabia, [13]University of Monastir, Faculty of Science of Monastir, Avenue of the Environment, 5019 Monastir, Tunisia, [14]Department of Chemistry, Faculty of Science and Arts of Baljurashi, Albaha University, Saudi Arabia, [15]Faculty of Science of Sfax, Department of Chemistry, University of Sfax, B.P. 1171, 3000 Sfax, Tunisia

ABSTRACT

Background: *Tabebuia impetiginosa* is an important medicinal plant rich in lapachol, α-lapachone, and β-lapachone known to possess several biological activities. **Objective:** In this study, we investigated the drug potential of lapachol, α-lapachone, and β-lapachone using molecular docking, molecular dynamic (MD), and drug-likeness properties. **Materials and Methods:** The computational study was performed using SwissADME software for the determination of the pharmacokinetic properties of the tested compounds. AutoDock Vina and Genetic Optimization for Ligand Docking (GOLD) were used for the docking analysis, and MD simulations were run using Schrodinger's Desmond Simulation. **Results:** The three compounds lapachol, α-lapachone, and β-lapachone binds to cysteine (Cys)-histidine (His) catalytic dyad (Cys145 and His41) along with the other residues with, respectively, the following docking score 48.69, 47.06, and 47.79. Against viral entry receptor, human angiotensin-converting enzyme 2 (hACE-2), α-lapachone exhibited the highest GOLD Fitness score complex (54.82) followed by lapachol (42.53) and β-lapachone and hACE-2 (38.74) generating several active sites in the target proteins. A 100 ns MDs simulation study revealed the stable conformation of bioactive compounds within the cavity of severe acute respiratory syndrome coronavirus 2 (SARS-CoV-2) of hACE-2 protein and main protease (Mpro). From the dynamic study, it was observed that lapachol was tightly bound with catalytic dyad residue Cys145 of Mpro with more than 40% time of simulation, also post-simulation MM-GBSA binding free energy (ΔG Bind) revealed the highest energy score (−51.18 ± 5.14 kcal/mol) among the evaluated complex. Moreover, the absorption, distribution, metabolism, and excretion (ADME) properties demonstrated that the investigated compounds passed the pharmacokinetic and drug-likeness criteria without undesirable effects. **Conclusion:** The computational study highlighted that these compounds could be highly recommended and developed as part of an effective drug against the SARS-CoV-2 virus.

Key words: Computer-aided strategies, drug repurposing, hACE-2, Mpro, SARS-CoV-2

SUMMARY

• Three natural bioactive compounds, namely, lapachol, α-lapachone, and β-lapachone isolated from *T. impetiginosa* were screened for their potential use as a promising candidate for COVID-19 Mpro and hACE-2 by using in silico approaches.

Docking analyses Dynamic study

Main protease: SARS-CoV-2 hACE2
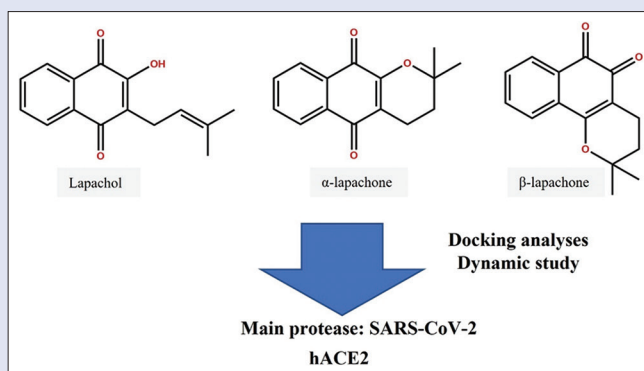
Abbreviations used: 2D: Two dimensional; 3D: Three dimensional; 3CLpro: 3-chymotrypsin like protease; Mpro: Main protease; ADME: Absorption, Distribution, Metabolism, and Excretion; COVID: Coronavirus Disease; SARS-CoV-2: Severe acute respiratory syndrome coronavirus 2; hACE-2: human Angiotensin-converting enzyme 2; TMPRSS2: Transmembrane Serine Protease 2; Cys: Cysteine; His: Histidine; GOLD: Genetic Optimisation for Ligand Docking; Autodock: Automatic Docking; MM-GBSA: Molecular Mechanics-Generalized Born Surface Area: rG: Radius Giration; RMSD: Root Mean Square Deviation; RMSF: Root Mean Square Fluctuation.

Correspondence:

Prof. Mejdi Snoussi,
Department of Biology, University of Hail, College of Science, P.O. Box 2440, Ha'il 2440, Saudi Arabia.
E-mail: snmejdi@yahoo.fr
DOI: 10.4103/pm.pm_251_22

Access this article online
Website: www.phcog.com
Quick Response Code:

INTRODUCTION

Plant-based secondary metabolites are potent reservoirs with many therapeutic and pharmacological effects.[1-4] They have attracted great attention due to their secreted bioactive molecules that could be developed as powerful drugs against several diseases without or with less side effects.[5-8] The consumption of herbal medicine is also known to improve the immune response.[9,10] Currently, the arsenal of antiviral and antibiotic drugs has been strictly compromised by the earlier devastating of COVID-19, forcing the creation of a new front-line for discovering effective drugs and new vaccines.[11,12] Severe acute respiratory syndrome coronavirus 2 (SARS-CoV-2) enters into host epithelial and lung cells by the interaction of spike protein to angiotensin-converting enzyme 2 (ACE-2) receptors using the cellular serine protease transmembrane serine protease 2 (TMPRSS2) for S protein priming.[13-15] The receptor binding domain in S1 directly binds to the peptidase domain of human angiotensin-converting enzyme 2 (hACE-2).[16]

During this epidemic, cancer patients are more exposed to infections and therefore are considered to be a highly vulnerable group. A literature survey outlined that the antiviral mechanism of lapachol and its derivatives have not been yet studied, but we inspired the use of lapachol and its analogs based on other studies using the anticancer drug on SARS-CoV-2, which enhances the body's immune response against cancer, were actually to treat COVID-19.[17] Also, β-lapachone as a pro-drug, with the commercial name ARQ-761, is actually in phase I/II of clinical studies for solid tumors.[18]

In silico docking, analysis has demonstrated that plant-derived molecules were able to bind to SARS-CoV-s main proteases two proteases [PLpro and 3-chymotrypsin like protease] responsible for the synthesis and maturation of the various viral polyproteins.[19] In 2020, Nayak[20] reviewed the interaction of peptidic and non-peptidic molecules with hACE-2 as potential inhibitors of SARS-CoV-2 attachment to human cells. It has been recently reported that linolenic and eicosapentaenoic acids highly block the entry of SARS-CoV-2 to the host cells.[21] Wang and colleagues[22] claimed that dalbavancin as a lipoglycopeptide antibiotic, directly binds to hACE-2, with high affinity, thereby blocking its interaction with the SARS-CoV-2 spike protein. Telmisartan (ClinicalTrials.gov ID: NCT04355936) and losartan (ClinicalTrials.gov ID: NCT04312009) were proposed as alternative options for treating COVID-19 patients before the development of acute respiratory distress syndrome.[23] Recently, Alacepril and lisinopril were found to interact with hACE-2.[24] Moreover, dermaseptin-S9 was able to prevent the attachment of SARS-CoV-2 spike protein to the surface of the ACE-2 receptor.[25] Besides that, alatrofloxacin, azithromycin, cefoperazone, rifapentine, and vancomycin as antibacterial drugs have been proved to bind to ACE-2 to obstruct SARS-CoV-2 binding.[26] Recent studies also reported the binding of nystatin and posaconazole against SARS-CoV-2 spike protein binding site.[27] On the other hand, the antihypertensive (Azilsartan kamedoxomil, deserpidine, and reserpine), statins (Pitavastatin and simvastatin), antimigraine (Dihydroergotamine), antiasthmatic (Zafirlukast), antihistamine (Loratadine), cardiac glycoside (Digoxin), and antimalarial (Mefloquine). Mefloquine (an antimalarial drug) has been confirmed to compete with spike protein for binding to ACE-2, rather than hydroxychloroquine, which binds to another region of ACE-2.[28,29] Other small molecules with anti-inflammatory actions like mycophenolic acid, pemirolast, isoniazid, and eriodictyol were also tested and demonstrated their good binding affinity to ACE-2, suggesting their importance in the treatment of COVID-19.[30]

Till now, no specific drugs for COVID-19 are available despite some vaccines that have been commercialized by different pharmaceutical companies, but there are controversies on the side effects. In addition, the gravity of the situation requires the use of all resources to remedy which scourge to find out therapeutic agents valid for a long period. Therefore, lapachol, α-lapachone (1,2-naphthoquinone), and β-lapachone (1,4-naphthoquinone) [Figure 1] as three natural products belonging to the naphthoquinone's classes.[31] Lapachol isolated from the heartwood of *Tabebuia impetiginosa* (syn. *T. avellanedae*) with the red type is known to cure several diseases such as herpes, malaria, cancer, fevers, eczema, ulcers, skin disorders, manage trypanosomiasis, syphilis, bacterial, and fungal infections.[32,33] Lapachol has been found to possess antiviral activity against Epstein–Barr virus and enterovirus *in vitro*.[34,35] Also, it has been reported that β-lapachone promotes the preparation of collagens and is responsible of whitening skin and hyperpigmentation skin diseases.[36,37] Both α-lapachone and β-lapachone represent significant cytotoxicity on mammalian cells and were used as a potential leishmanicidal drug.[38] β-Lapachone has been described to prevent the proliferation of cancer cells, to inhibit human lung cancer xenograft growth and angiogenesis, used as pro-drug, with commercial name ARQ-761, is in phase I/II of clinical studies for solid tumors as well as to promote various biological properties including anti-inflammatory, antibacterial, and anti-trypanosoma.[31,38-40]

Therefore, in the present study, we investigated lapachol, α-lapachone, and β-lapachone as potential inhibitor candidates for COVID-19 main protease (Mpro) and hACE-2, using modeling, virtual screening, molecular docking, and molecular dynamics (MDS) simulation with absorption, distribution, metabolism, and excretion (ADME) and target prediction.

MATERIALS AND METHODS

Molecular docking

Three-dimensional (3D) structure of 6LU7 and 2AJF was retrieved from RCSB Protein Data Bank.[39]

Docking using autoDock Vina and Genetic Optimization for Ligand Docking (GOLD)

Docking of protein ligands was carried out using AutoDock Vina,[40] GOLD,[41,42] and LibDock from Discovery Studio Client v20.1.0.19295. The receptor protein 6LU7 was prepared by removing water and co-crystal ligand (remdesivir), hydrogen and charges were added to the structures. The grid box dimensions as follow: $x = -10.729$ Å, $y = 12.418$ Å, $z = 68.816$ Å and grid box size as follows: $x = 50$ Å, $y = 50$ Å, $z = 50$ Å were set for 6LU7 a grid space of 0.375 Å. The ligand pdbqt file was prepared in AutoDock MG Tool. During the docking process, the ligand was kept flexible and receptors were set rigid.

Molecular dynamic (MD) simulation

Molecular docking studies predict ligand binding status in rigid protein structures (static conditions). Therefore, MD simulations were run using Schrodinger's Desmond Simulation as done previously.[43-48]
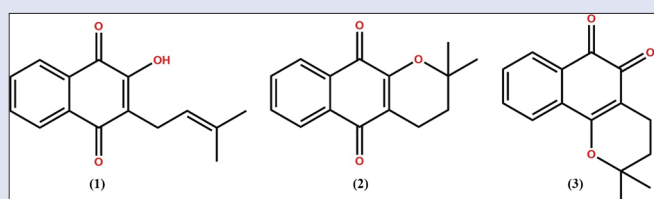

Figure 1: Structures of lapachol (1), α-lapachone (2) and β-lapachone (3)

Post-simulation molecular mechanics-generalized born surface area (MM-GBSA) analysis

Post-simulation binding free energies (ΔG Bind) of the ligand–protein complexes were calculated using the molecular mechanics combined with a generalized MM-GBSA approach. The Python script thermal_mmgbsa.py was employed to assess Prime MM-GBSA binding free energy for 0–1000 frames having a 100-step sampling size in the simulation trajectory with the VSGB solvation model associated with the OPLS3e force field. VSGB is a novel energy model (VSGB 2.0) for high resolution protein structure modeling. The Prime MM-GBSA binding free energy (kcal/mol) is calculated following the same work of Patel *et al*.[49]

ADMET and molecular target predictions

Pharmacokinetic assessment of lapachol, α-lapachone, and β-lapachone was performed using SwissADME[50-53] and pkCSM web tools.[54]

RESULTS

Binding Interaction of Lapachol, α-Lapachone, and β-Lapachone with Mpro

Molecular docking of the selected known bioactive compounds was performed to study their interaction mode against SARS-CoV-2 Mpro (PDB ID: 6LU7) and hACE-2 (PDB ID: 2AJF). Figure 2 shows the binding affinities along with the neighboring residues of papain-like protease (PLpro) and human receptor protein hACE-2 interacting with the selected compounds.

The three compounds lapachol, α-lapachone, and β-lapachone bind to cysteine (Cys)-histidine (His) catalytic dyad (Cys145 and His41) along with the other residues with, respectively, the following docking score 48.69, 47.06, and 47.79. Lapachol forms one H-bonds with Glu143 and other hydrophobic interactions. α-Lapachone established van der Waals interactions with Tyr54, Cys145, His164, Glu166, Leu167, Pro168, Val186, Asp187, Thr190; H-bond: Gln192; Unfavorable Bump interaction with only Arg188, Pi-Sigma interactions with Gln189 and

Alkyl/Pi-Alkyl interactions with His41, Met49, and Met165 residues, however, β-lapachone binds to Mpro residues *via* several hydrophobic interactions.

Binding interaction of Lapachol, α-Lapachone, and β-Lapachone with hACE-2

The obtained data of docked complexes between the selected molecules and the crystal structure of hACE-2 unveiled that lapachol expressing high binding score was found to interact with binding pockets to form hydrophobic interactions with Glu310, Lys313, Phe314, Ser317, Lys416, His417, Ser420, Ile421, Ser545, Asn546, and Asp543 amino acids. α-lapachone-hACE-2 complex (54.82) generated van der Waals interactions with Ser420, Asp543, Ile544, and Ser547. The other significant interactions that stabilize α-lapachone and hACE-2 complex include Pi-Lone Pair with Ser545, C-H bonds with Ser545, Amide-Pi Stacked interactions with Asn546, and Alkyl/Pi-Alkyl with Lys416, His417, Ala533. The highest binding energy between β-lapachone and hACE-2 established H bonds interactions with Lys416, van der Waals interactions with His417, Ser420, Cys530, Lys534, His535, Asp543, Ile544, Asn546, Ser547, Pi-Lone Pair interaction with Ser545, and Alkyl/Pi-Alkyl with Ala533, Cys542 residues.

Molecular dynamics simulation

In order to understand the stability and conformations changes of the hACE-2 protein (2AJF) and Mpro (6LU7) domain complexed with the bioactive compounds lapachol and α/β-lapachone, we performed the root mean square deviation (RMSD), root mean square fluctuations (RMSF), protein–ligand contact mapping and the time-dependent radius of gyration (rGyr).[49,55] The RMSD value for the Cα atoms was computed over 100 ns simulations to evaluate the stability of all the systems. Lower the RMSD fluctuation infers a more stable structure of the protein. The RMSD plot of simulated complex is presented in Figure 2. The simulation results of the 2AJF-β-lapachone complex showed that ligand has crossed the RMSD value of more than 4 Å (acceptable RMSD 1–3)
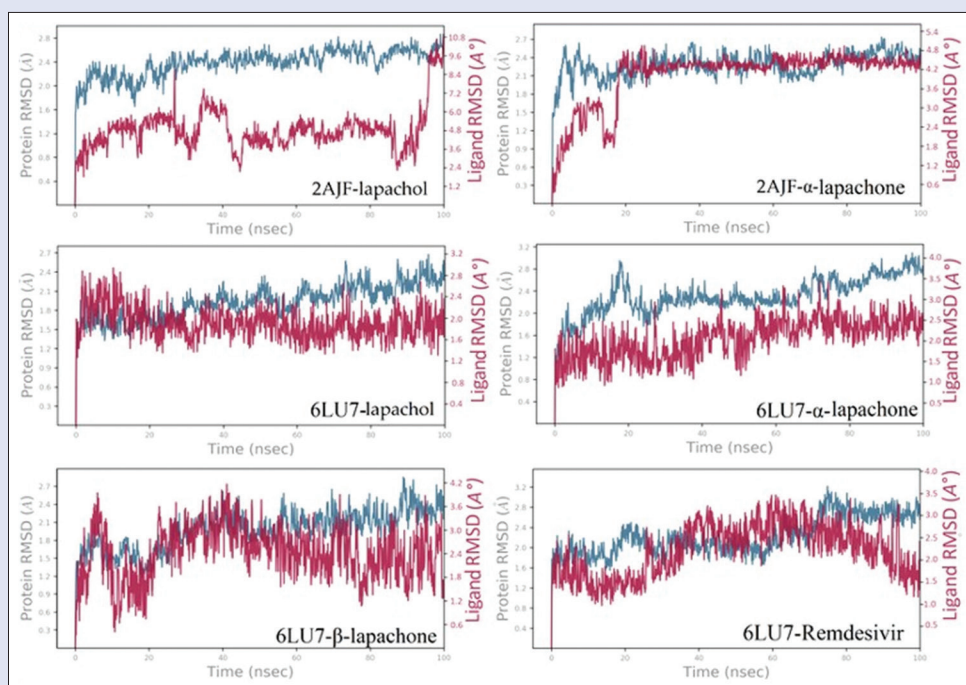

Figure 2: Time decedent RMSD of Simulated protein–ligand complex (Protein–RMSD is shown in gray while RMSD of Ligand is shown in red)

and was found unstable during the 100 ns time of the simulation. The RMSD of the 2AJF-α-lapachone, 6LU7-lapachol, 6LU7-α-lapachone, and 6LU7-β-lapachone was observed to be 4.2 Å, 2.4 Å, 3.0 Å, and 3.5 Å, respectively, as compared to the initial structure (zero frame ligand). Slightly higher RMSD was observed for the 2AJF lapachol at around 96 ns as shown in Figure 3. In the 2AJF-β-lapachone complex, the highest fluctuation was observed at a time span of 91 ns with an RMSD of 3.6 Å. To assess remdesivir stability in complex with SARS CoV-2 main protease, the RMSD value for the Cα backbone was monitored for 100 ns simulations.

During the simulation, the flexibility of the protein system was also examined by computing the RMSF of individual amino acid residues in the protein to examine the binding efficiency of bioactive compounds with hACE-2 and Mpro proteins [Figure 3]. The average RMSFs assessed for the complex of 2AJF-Lapachol, 2AJF-α-lapachone, 6LU7-Lapchol, 6LU7-α-lapachone, and 6LU7-β-lapachone and 6LU7-remdesivir are 1.123 Å, 0.893Å, 0.921 Å,1.094 Å, 1.777 Å, and 1.245 Å, respectively, that implying that hACE-2 protein and Mpro protein exhibit minimal fluctuation and relative secondary conformational stability upon binding of reported bioactive compounds.[56-59] All the RMSF values in Å of ligand contacted residues are listed in Table 1.

Throughout the simulation, protein interactions with the ligand were also monitored. These interactions can be categorized by type, reviewed, and portrayed in Figure 4. The amino acid residues Asn546 and Lys313 of hACE-2 exhibited hydrogen bond and water-mediated hydrogen bond interactions with the Lapachol, as revealed by docking studies, which also existed in MD throughout the trajectory, with 46 and 64% interaction of stipulated time. The second bioactive compound α-lapachone on target 2AJF revealed significant hydrophobic interaction with hydrophobic amino acid residues Pro321 and Phe555, during the entire simulation. Apart from these residues, amino acid Val318, Gly319, Asp543, Asn546, Ser547, and Arg559 also contributed to the water-mediated hydrogen bond with the target molecule in the active site. It is noticed that

simulated bioactive compound (Lapachol and α-lapachone) in 2AJF Protein mostly interacted through hydrophobic and water-mediated hydrogen bonding.

It was observed [Figure 2] that lapachol interacted with the Mpro active site with Gly143, Ser144, and Gln189 mainly through hydrogen bonding with 29–86% throughout the simulation time. A crucial catalytic dyad residue, Cys145, was also actively contributed by a bidentate hydrogen bond with Lapachol in the active site. The terminal carbonyl group of α-lapachone interacted with Thr190 (35%) and Gln192 (53%) via hydrogen bonding. Active site amino acid residues of 6LU7 like Asn142, Cys145, His164, Glu166, and Gln189 were also contacted with α-lapachone through water-mediated hydrogen bonding. In the complex of β-lapachone-Mpro, mainly hydrophobic and water-mediated hydrogen bond interactions were observed. In this complex, crucial residue Cys145 interacts with β-lapachone via three types of interaction, hydrogen bonding, hydrophobic, and water-mediated hydrogen bonding. Protein–ligand contact mapping shows that remdesivir binds to the main protease protein through Thr25, Thr45, Asn142, Gly143, Cys145, Glu166, Gln189, and Thr190 and exhibited more than 10% hydrogen bond interactions. Among them, catalytic dyed residue Cys145 makes all three (hydrogen, hydrophobic, and water-mediated hydrogen bonding) types of interaction with remdesivir [Figure 4].

The rGyr property was also investigated to demonstrate the stability of the bioactive compounds in the hACE-2 protein and Mpro binding pockets over a 100 ns simulation. The extension of a ligand is estimated by its rGyr, which is comparable to its principal moment of inertia [Figure 5]. A high value or abnormal variation of rGyr in different frames signifies the instability of the system, whereas a low and consistent variation of rGyr indicates the stability of the system. The bioactive compounds in complexes with hACE-2 protein and Mpro exhibited an average rGyr value of 3 Å [Table 2]. The rGyr did not show any significant changes. These constant values exhibited a consistent pattern of behavior.
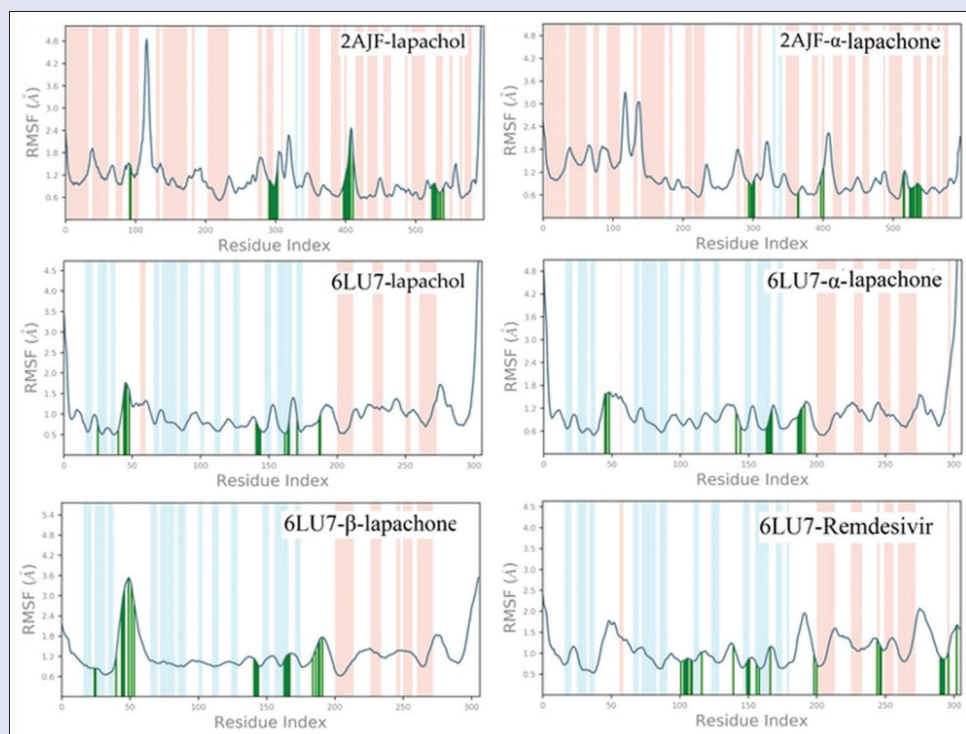

Figure 3: The RMSF of Cα atoms of hACE-2 protein (2AJF) and M^{pro} (6LU7)

Table 1: RMSF values *Cα* atoms of ligand contacted residues with hACE-2 protein (2AJF) and Mpro protein (6LU7) after binding of lead compounds

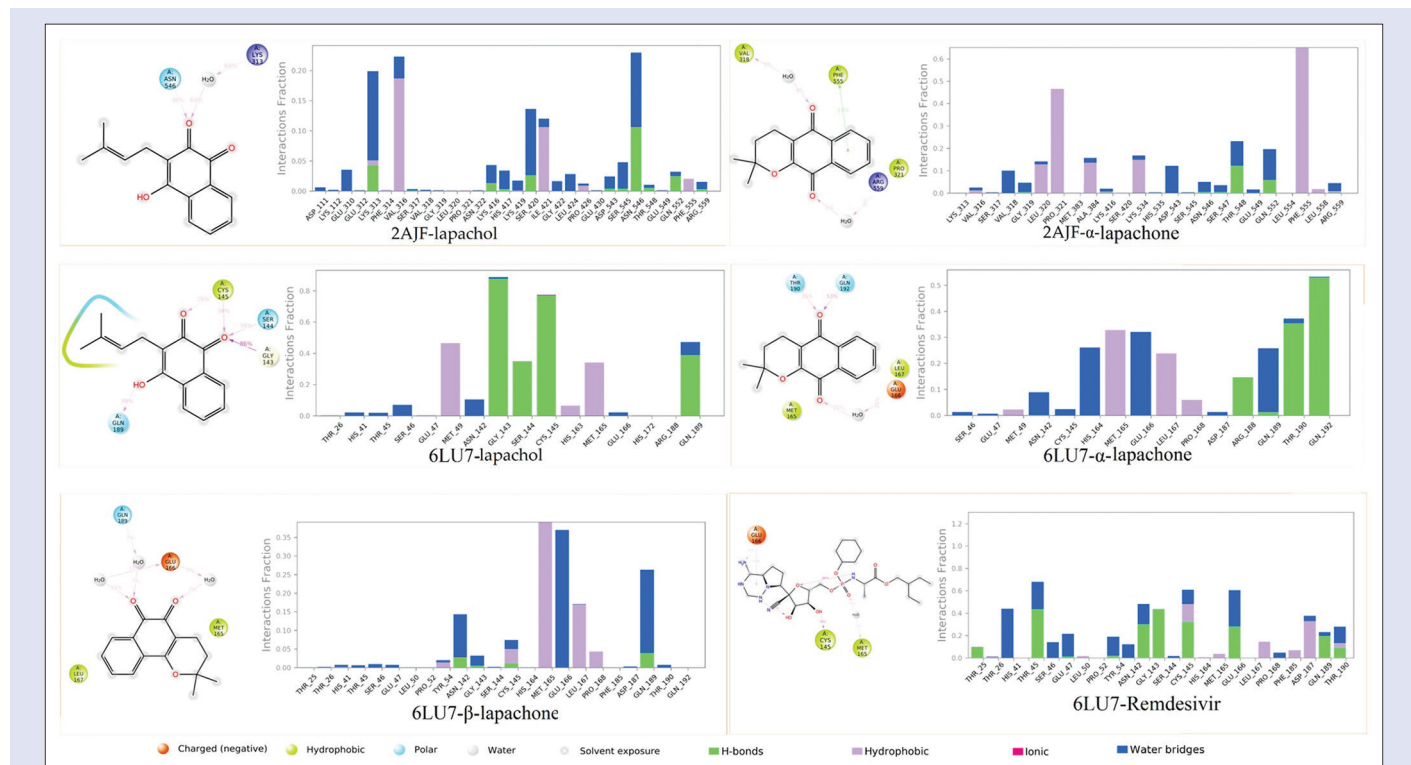| hACE-2 protein (2AJF).				SARS-CoV-2 Mpro (6LU7)					
Lapchol Complex	RMSF (A°)	α-Lapchone Complex	RMSF (A°)	Lapchol Complex	RMSF (A°)	α-Lapchone Complex	RMSF (A°)	β-Lapchone Complex	RMSF (A°)
Asp111	1.747	Lys313	0.987	Thr26	0.717	Ser46	Ser46	Thr25	1.024
Lys112	1.261	Val316	0.858	His41	0.582	Glu47	Glu47	Thr26	0.825
Glu310	1.042	Ser317	0.869	Thr45	1.528	Met49	Met49	His41	0.821
Glu312	1.088	Val318	0.767	Ser46	1.68	Asn142	Asn142	Thr45	2.684
Lys313	1.114	Gly319	0.859	Glu47	2.239	Cys145	Cys145	Ser46	3.493
Phe314	0.851	Leu320	0.788	Met49	1.121	His164	His164	Glu47	4.548
Val316	0.905	Pro321	0.847	Asn142	0.875	Met165	Met165	Leu50	4.511
Ser317	0.891	Met383	0.601	Gly143	0.747	Glu166	Glu166	Pro52	3.163
Val318	0.894	Ala384	0.614	Ser144	0.603	Leu167	Leu167	Tyr54	2.094
Gly319	0.964	Lys416	1.168	Cys145	0.498	Pro168	Pro168	Asn142	1.31
Leu320	0.952	Ser420	1.395	His163	0.507	Asp187	0.788	Gly143	1.112
Pro321	1.305	Lys534	1.138	Met165	0.532	Arg188	1.169	Ser144	0.832
Asn322	1.603	His535	1.602	Glu166	0.631	Gln189	1.198	Cys145	0.784
Lys416	0.98	Asp543	0.732	His172	0.626	Thr190	1.263	His164	0.838
His417	0.925	Ser545	0.915	Arg188	0.859	Gln192	1.05	Met165	0.961
Lys419	1.173	Asn546	0.804	Gln189	0.997	Glu166	Glu166	Glu166	1.041
Ser420	1.321	Ser547	0.725			Leu167	Leu167	Leu167	1.416
Ile421	1.416	Thr548	0.818			Pro168	Pro168	Pro168	1.818
Gly422	1.472	Glu549	0.791					Phe185	1.012
Leu424	1.48	Gln552	0.893					Asp187	1.081
Glu430	1.808	Leu554	0.854					Gln189	1.745
Asp543	0.971	Phe555	1.02					Thr190	1.869
Ser545	1.089	Leu558	0.668					Gln192	1.892
Asn546	1.009	Arg559	0.707						
Thr548	1.002								
Glu549	0.869								
Gln552	0.766								
Phe555	0.772								
Arg559	0.892								

Figure 4: Protein–ligand contact analysis of MD trajectory, monitored throughout the 100 ns simulation time

The MM-GBSA method uses molecular mechanics, generalized Born solvation models, and a solvent accessibility approach to estimate binding free energies (ΔG Bind) based on MD simulation trajectories. The post-simulation MM-GBSA was calculated from frame 0 to 1000

at every 10th frame, totaling 100 structures of each protein–ligand complexes, and average binding energies with standard deviation have been tabulated in Table 2. The calculated average ΔG Bind of the complex of 2AJF-Lapachol, 2AJF-α-lapachone, 6LU7-Lapchol, 6LU7-α-lapachone, 6LU7-β-lapachone, and 6LU7-remdesivir was found to be − 24.9477 kcal/mol, −34.0672 kcal/mol, −51.1813 kcal/mol, −42.1107 kcal/mol, −39.3305 kcal/mol, and − 46.50 kcal/mol, respectively, (49,50). 6LU7-Lapchol results displayed the promising binding free energy scores when compared with the remdesivir complex MM-GBSA calculations.

ADME properties

Assessment of pharmacokinetic possessions for a successful drug in the early phases of drug discovery and development through *in silico* ADME screens is essential to achieve their drug-likeness and minimize their risk attrition in the late stage. Results [Table 3] showed good drug-likeness properties and that the selected compounds could not be substrates of P-glycoprotein (P-gp). The cytochrome P450 monooxygenase (CYP) enzymes super-family regrouping cytochrome CYP1A2, CYP2C19, CYP2C9, CYP2D6, and CYP3A4 are important in drug metabolism in the liver and biotransformation of drugs through O-type oxidation reactions have been predicted, especially those of 2D6, 2C9, and 3A4

Figure 5: Radius of gyration (rGyr) graph of the simulated complex at 100 ns simulation time

which are the most important forms in human. Data showed that all hits are inhibitors of CYP1A2 and CYP2C19, not inhibitors of CYP2C9 and CYP2D6; however, CYP3A4 was only inhibited by β-lapachone. The selected compounds exhibited good lipophilicity results with a bioavailability score (85%) and suitable skin permeation (LogK$_p$) values suggesting making them easily accessible *via* the skin.

The pink area of bioavailability radar chart of three compounds [Figure 6] representing the most drug-likeness parameters justified that the designed compounds are fully included in the pink area suggesting their good oral bioavailability.

BOILED-Egg graph (WLOGP *vs.* TPSA) indicates that the three molecules are non-substrate of P-gp [Figure 7].

Target prediction

Data [Figure 8] outlined that lapachol has 26% enzyme, 12% protease, and 4% of kinase, whereas α-lapachone predicts 18% enzyme, 20% protease, and 2% of kinase and β-lapachone can be targeted for 26% enzyme and 4% of the kinase.

DISCUSSION

This study aimed to screen three bioactive molecules, lapachol, α-lapachone, and β-lapachone identified in the medicinal plat, *T. impetiginosais* that can target Mpro and hACE-2 to find novel compounds that can be used as a new drug against coronavirus as a strategy in antiviral drug discovery and development.[60] Results were confirmed when compared to the residues of the high-volume pocket of Mpro sharing more identical amino acids. Lapachol, α-lapachone, and β-lapachone also show high binding efficiencies suggesting their high potential for repurposing. Recently, different synthetic drugs were docked with SARS-CoV-2 proteins including hydroxychloroquine, chloroquine, ivermectin, raltegravir, daclatasvir, simeprevir, cobicistat, oseltamivir, and remdesivir demonstrated that drug molecules of oseltamivir, ritonavir, remdesivir, ribavirin, and favipiravir had a greater capability to inhibit SARS-CoV-2, since they demonstrated high-affinity interactions with the COVID-19 Mpro in complex with the N3 inhibitor.[60-62]
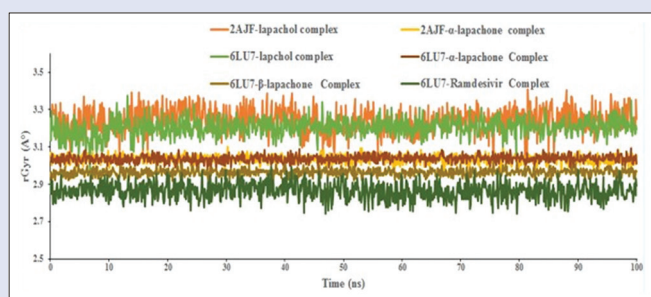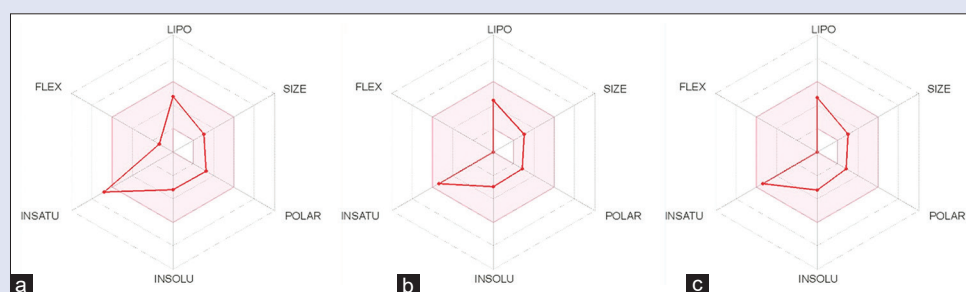

Figure 6: Bioavailability radar of the selected compounds, based on their physicochemical indices ideal for the oral bioavailability. (a) Lapachol; (b) α-Lapachone ; (c) β-Lapachone

Table 2: Radius of gyration of and post-simulation MM-GBSA-based binding free energy (ΔG Bind) for the protein–ligand complexes

Complex name	Radius of gyration, rGyr (A°)		MM-GBSA, ΔG Bind (kcal/mol)	
	Mean	Range	Mean	Range
2AJF-Lapachol	3.24±0.06	3.41 to 3.02	−24.95±4.35	−30.86 to−17.98
2AJF-α-lapachone	3.03±0.02	3.10 to 2.96	−34.07±9.11	−45.57 to−18.57
6LU7-Lapchol	3.20±0.05	3.38 to 2.97	−51.18±5.14	−56.32 to−39.69
6LU7-α-lapachone	3.03±0.02	3.09 to 2.96	−42.11±4.40	−50.36 to−33.86
6LU7-β-lapachone	2.96±0.02	3.02 to 2.91	−39.33±4.91	−46.26 to−28.83
6LU7-β-remdesivir	2.86±0.05	2.72 to 3.00	−46.50±3.96	−59.12 to−38.27

In order to validate our results, the viral RNA polymerase inhibitors, remdesivir have been also docked against 6LU7 and compared to lapachol, α-lapachone, and β-lapachone. Results showed that remdesivir interacts with 6LU7 forming the following interactions: H-bond with Glu166 (2.38 Å), Gln189 (2.63 Å); Carbon H-bond with Thr190 (1.86 Å); Pi-Anion with Glu166 (4.26 Å) and Alkyl/Pi-Alkyl with His41 (4.05 Å), Met49 (3.75 Å), and Ala 191 (4.34 Å) residues [Figure 9]. Based on the above data, lapachol, α-lapachone and β-lapachone shared several residues as remdesivir when interacting with 6LU7, especially those of His41, Met49, Glu166, and Gln189 (lapachol), and His41, Met49, Glu166, Gln189, and Thr190 (α-lapachone and β-lapachone). Thus lapachol, α-lapachone, and β-lapachone hold the potential to be developed as treatment toward COVID-19.

Previous reports have investigated the interaction between plant-derived compounds and marine-based molecules with SARS-CoV-2 key enzymes.[63-70] In 2020, Bhuiyan and colleagues[61] reported that about 219 plants belonging to 83 families with antiviral activities, and among them 149 plant species (from 71 families) possess several secondary metabolites (glycosides, flavonoids, alkaloids, tannins, saponins, phenolic acids, terpenoids, coumarins, organosulfur compounds, nitrogen-containing compounds, etc.) that can interfere with SARS-CoV-2 enzymes. Using computational approaches (molecular docking and dynamic simulation), Maurya and Sharma[71] demonstrated that traditional Kadha preparation (Ayurvedic medicine) possesses diverse phytoconstituents that can be useful for the treatment and prevention of COVID-19 virus as they showed high binding affinity (low binding energy). The same authors reported that withaferin A (−9.1 kcal/mol), stigmasterol (−8.8 kcal/mol), vicenin (−8.8 kcal/mol), and ursolic acid (−8.7 kcal/mol) were the highest molecules binding to hACE-2.

A 100 ns molecular dynamics simulation study showed the stable conformation of bioactive compounds within the cavity of hACE-2 protein and Mpro. From the dynamic study, it was assumed that the promising bioactive compound lapachol has been tightly bound with catalytic dyad residue Cys145 of Mpro with more than 40% time of simulation, also post-simulation MM-GBSA binding free energy (ΔG Bind) revealed the highest energy score (−51.18 ± 5.14 kcal/mol) among the evaluated complex.

All these findings highlighted the potential use of natural compounds from medicinal and aromatic plant extract as SARS-CoV-2 inhibitors.
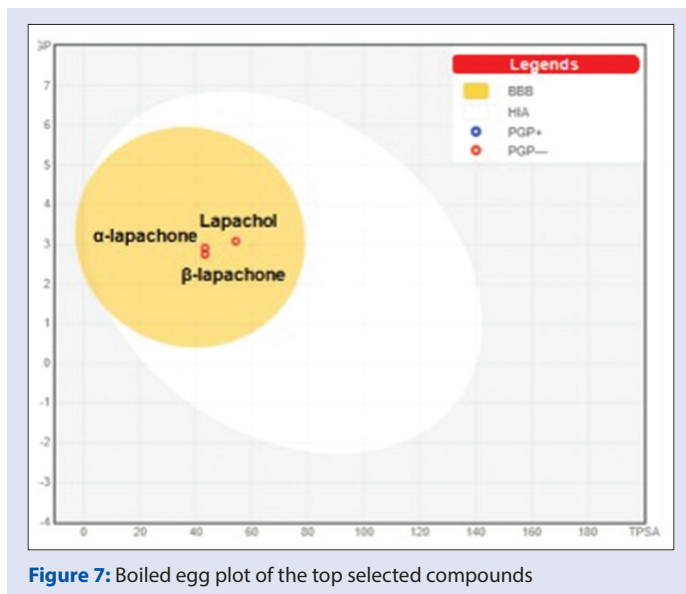

Figure 7: Boiled egg plot of the top selected compounds

Table 3: ADME profiles of lapachol, α-lapachone and β-lapachone according to SwissADME software

| Entry	Lapachol	α-lapachone	β-lapachone
GI absorption	High	High	High
BBB permeant	Yes	Yes	Yes
P-gp substrate	No	No	No
CYP1A2 inhibitor	Yes	Yes	Yes
CYP2C19 inhibitor	Yes	Yes	Yes
CYP2C9 inhibitor	No	No	No
CYP2D6 inhibitor	No	No	No
CYP3A4 inhibitor	No	No	Yes
Log Kp (skin permeation)	−5.80	−6.22	−5.90
Lipinski	Yes	Yes	Yes
Bioavailability Score	0.85	0.85	0.55
Consensus Log P$_{o/w}$	2.54	2.42	2.56
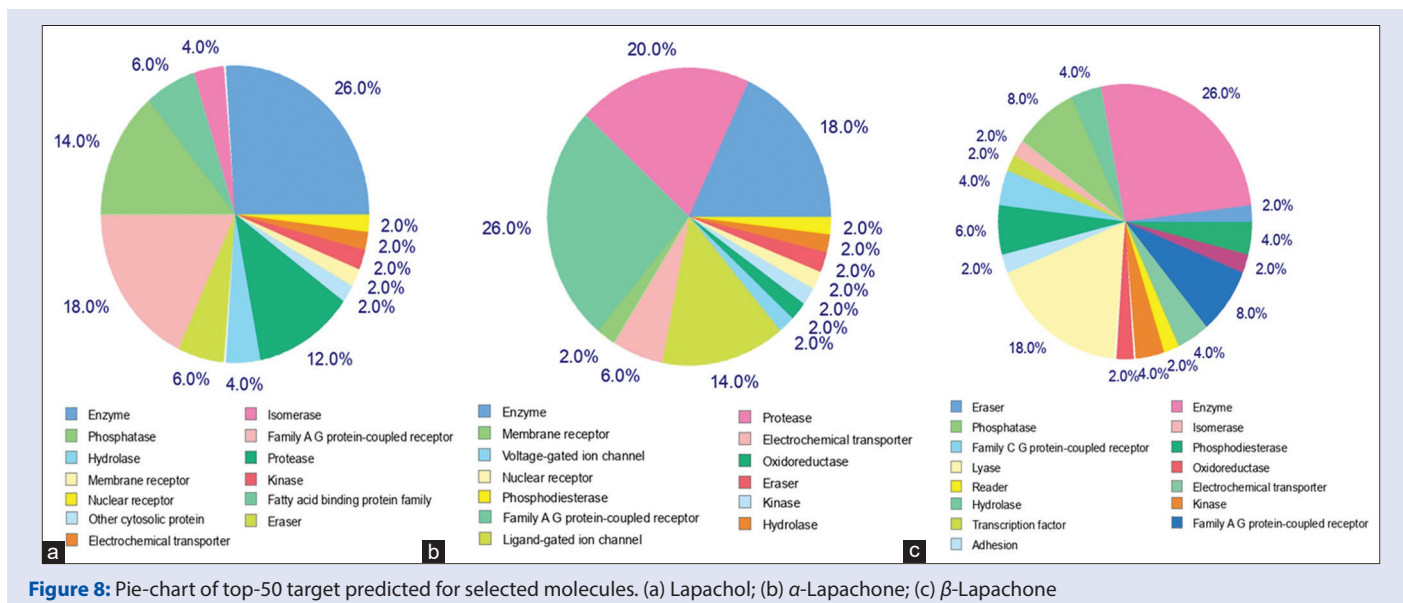
Figure 8: Pie-chart of top-50 target predicted for selected molecules. (a) Lapachol; (b) α-Lapachone; (c) β-Lapachone
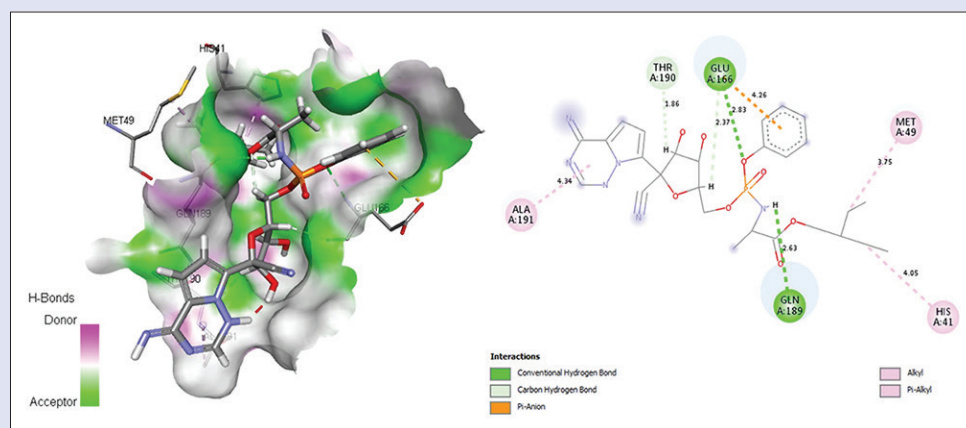
Figure 9: GOLD Fitness docking score, 2D, 3D, and interacting residues of remdesivir with the active site of COVID-19 6LU7 (M^{pro}). AutoDock Vina Docking Score: remdesivir-6LU7 (-7.8 kcal/mol); Residues interacting with compounds: Conventional hydrogen bond: Glu166 (2.38 Å), Gln189 (2.63 Å); Carbon hydrogen bond: Thr190 (1.86 Å); Pi-Anion: Glu166 (4.26 Å); Alkyl/Pi-Alkyl: His41 (4.05 Å), Met49 (3.75 Å), Ala 191 (4.34 Å)

CONCLUSION

In this study, we have demonstrated the potential of lapachol, α-lapachone, and β-lapachone as main ligands for the SARS-CoV-2 and that SARS-CoV-2 Mpro and hACE-2 may be a viable target for antiviral development. Molecular dynamics simulations were performed on protein–ligand complex using Desmond at 100 ns to investigate their binding conformational stability. The stability of the protein–ligand complex was observed to be maintained throughout the 100 ns simulations based on RMSD, RMSF, and protein–ligand interactions. Also, all the amino acid interactions identified during docking studies of the bioactive compounds were also shown during the dynamic simulation study. Especially, lapachol was found that have tightly bound to Mpro crucial residue Cys145 with a significant −51.1813 ± 5.14 kcal/mol ΔG Bind score. As per pharmacokinetics investigation, the compounds showed excellent drug-likeness properties. This study shows the effectiveness and importance of studying protein–ligand complex stability via dynamics to corroborate docking studies. Furthermore, these bioactive molecules would have the potential to act as promising drug candidates and could be utilized for further investigations as a template against SARS-CoV-2 with mandatory *in vitro* assays, before their evaluation in patients through clinical trials.

Our work shows the importance of studying protein–ligand complex stability via dynamics to corroborate docking studies. Although the results seem promising, it is important to validate this activity. Therefore, these molecules should be further investigated for *in vitro* and/or *in vivo* antiviral activity. They may also be used as templates for the development of future drugs against SARS-CoV-2 and other coronaviruses. Thus, these data may provide relevant information to advance our ability to combat COVID-19.

Conflicts of interest

There are no conflicts of interest.

REFERENCES

1. Felhi S, Saoudi M, Daoud A, Hajlaoui H, Ncir M, Chaabane R, *et al.* Investigation of phytochemical contents, *in vitro* antioxidant and antibacterial behavior and *in vivo* anti-inflammatory potential of Ecballium elaterium methanol fruits extract. Food Sci Technol 2017;37:558-63.

2. Daoud A, Ben Mefteh F, Mnafgui K, Turki M, Jmal S, Ben Amar R, *et al.* Cardiopreventive effect of ethanolic extract of date palm pollen against isoproterenol induced myocardial infarction in rats through the inhibition of the angiotensin-converting enzyme. Exp Toxicol Pathol 2017;69:656-65.

3. Adil M, Baig MH, Rupasinghe HPV. Impact of citral and phloretin, alone and in combination, on major virulence traits of *Streptococcus pyogenes*. Molecules 2019;24:4237.

4. Felhi S, Hajlaoui H, Ncir M, Bakari S, Ktari N, Saoudi M, *et al.* Nutritional, phytochemical and antioxidant evaluation and FT-IR analysis of freeze-dried extracts of Ecballium elaterium fruit juice from three localities. Food Sci Technol 2016;36:646-55.

5. Adil M, Khan R, Rupasinghe HPV. Application of medicinal plants as a source for therapeutic agents against *Streptococcus pyogenes* infections. Curr Drug Metab 2018;19:695-703.

6. Adil M, Singh K, Verma PK, Khan AU. Eugenol-induced suppression of biofilm-forming genes in *Streptococcus mutans*: An approach to inhibit biofilms. J Glob Antimicrob Resist 2014;2:286-92.

7. Mseddi K, Alimi F, Noumi E, Veettil VN, Deshpande S, Adnan M, *et al.* Thymus musilii Velen. as a promising source of potent bioactive compounds with its pharmacological properties: *in vitro* and *in silico* analysis. Arab J Chem 2020;13:6782-801.

8. Bakari S, Hajlaoui H, Daoud A, Mighri H, Ross-Garcia JM, Gharsallah N, *et al.* Phytochemicals, antioxidant and antimicrobial potentials and LC-MS analysis of hydroalcoholic extracts of leaves and flowers of Erodium glaucophyllum collected from Tunisian Sahara. Food Sci Technol 2018;38:310-7.

9. Villamagna AH, Gore SJ, Lewis JS, Doggett JS. The need for antiviral drugs for pandemic coronaviruses from a global health perspective. Front Med (Lausanne) 2020;7:596587.

10. Bhatti JS, Bhatti GK, Khullar N, Reddy AP, Reddy PH. Therapeutic strategies in the development of anti-viral drugs and vaccines against SARS-CoV-2 infection. Mol Neurobiol 2020;57:4856-77.

11. Alminderej F, Bakari S, Almundarij TI, Snoussi M, Aouadi K, Kadri A. Antimicrobial and wound healing potential of a new chemotype from *Piper cubeba* L. essential oil and in silico study on S. aureus tyrosyl-tRNA synthetase protein. Plants (Basel) 2021;10:205-24.

12. Kadri A, Zarai Z, Ben Chobba I, Gharsallah N, Damak M, Bekir A. Chemical composition and *in vitro* antioxidant activities of *Thymelaea hirsuta* L. essential oil from Tunisia. Afr J Biotechnol 2011;15:2930-5.

13. Shang J, Wan Y, Luo C, Ye G, Geng Q, Auerbach A, *et al.* Cell entry mechanisms of SARS-CoV-2. Proc Natl Acad Sci U S A 2020;117:11727-34.

14. Llivisaca-Contreras SA, Naranjo-Morán J, Pino-Acosta A, Pieters L, Vanden Berghe W, Manzano P, *et al.* Plants and natural products with activity against various types of coronaviruses: A review with focus on SARS-CoV-2. Molecules 2021;26:4099.

15. Saadah LM, Deiab GIA, Al-Balas Q, Basheti IA. Carnosine to combat novel coronavirus (nCoV): Molecular docking and modeling to cocrystallized Host Angiotensin-Converting Enzyme 2 (ACE2) and viral spike protein. Molecules 2020;25:5605.

16. David AB, Diamant E, Dor E, Barnea A, Natan N, Levin L, *et al*. Identification of SARS-CoV-2 receptor binding inhibitors by *in vitro* screening of drug libraries. Molecules 2021;26:3213.

17. Gowrishankar S, Muthumanickam S, Kamaladevi A, Karthika C, Jothi R, Boomi P, *et al*. Promising phytochemicals of traditional Indian herbal steam inhalation therapy to combat COVID-19 – An *in silico* study. Food Chem Toxicol 2021;148:111966.

18. Connelly D. Targeting COVID-19: The drugs being fast-tracked through clinical trials and how they work. Pharm J 2020;304:312-3.

19. Remali J, Aizat WM. A Review on plant bioactive compounds and their modes of action against coronavirus infection. Front Pharmacol 2021;11:589044.

20. Nayak SK. Inhibition of S-protein RBD and hACE2 interaction for control of SARS-CoV- 2 infection (COVID-19). Mini Rev Med Chem 2021;21:689-703.

21. Goc A, Niedzwiecki A, Rath M. Polyunsaturated ω-3 fatty acids inhibit ACE2-controlled SARS-CoV-2 binding and cellular entry. Sci Rep 2021;11:5207.

22. Wang G, Yang ML, Duan ZL, Liu FL, Jin L, Long CB, *et al*. Dalbavancin binds ACE2 to block its interaction with SARS-CoV-2 spike protein and is effective in inhibiting SARS-CoV-2 infection in animal models. Cell Res 2021;31:17–24.

23. Alnajjar R, Mostafa A, Kandeil A, Al-Karmalawy AA. Molecular docking, molecular dynamics, and *in vitro* studies reveal the potential of angiotensin II receptor blockers to inhibit the COVID-19 main protease. Heliyon 2020;6:e05641.

24. Gurwitz D. Angiotensin receptor blockers as tentative SARS-CoV-2 therapeutics. Drug Dev Res 2020;81:537-40.

25. Al-Karmalawy AA, Dahab MA, Metwaly AM, Elhady SS, Elkaeed EB, Eissa IH, *et al*. Molecular docking and dynamics simulation revealed the potential inhibitory activity of ACEIs against SARS-CoV-2 targeting the hACE2 receptor. Front Chem 2021;9:661230.

26. Hakih TM. Dermaseptin-based antiviral peptides to prevent COVID-19 through in silico molecular docking studies against SARS-CoV-2 spike protein. Pharm Sci Res 2020;7:65-70.

27. Kim S, Chen J, Cheng T, Gindulyte A, He J, He S, *et al*. PubChem 2019 update: Improved access to chemical data. Nucleic Acids Res 2019;47:D1102-9.

28. Maffucci I, Contini A. In silico drug repurposing for SARS-CoV-2 main proteinase and spike proteins. J Proteome Res 2020;19:4637-48.

29. Ahsan T, Sajib AA. Repurposing of approved drugs with potential to interact with SARS-CoV-2 receptor. Biochem Biophys Rep 2021;26:100982.

30. Deshpande RR, Tiwari AP, Nyayanit N, Modak M. *In silico* molecular docking analysis for repurposing therapeutics against multiple proteins from SARS-CoV-2. Eur J Pharmacol 2020;886:173430.

31. Gerber DE, Beg MS, Fattah F, Frankel AE, Fatunde O, Arriaga Y, *et al*. Phase 1 study of ARQ 761, a β-lapachone analogue that promotes NQO1-mediated programmed cancer cell necrosis. Br J Cancer 2018;119:928-36.

32. Ferraz da Costa DC, Pereira Rangel L, Martins-Dinis MMDDC, Ferretti GDDS, Ferreira VF, Silva JL. Anticancer potential of resveratrol, β-lapachone and their analogues. Molecules 2020;25:893.

33. Hussain H, Green IR. Lapachol and lapachone analogs: A journey of two decades of patent research (1997-2016). Expert Opin Ther Pat 2017;27:1111-21.

34. Pinto AV, Pinto MDC, Lagrota MH, Wigg MD, Aguiar AN. Antiviral activity of naphthoquinones. I. Lapachol derivatives against enteroviruses. Rev Latinoam Microbiol 1987;29:15-20.

35. Sacau EP, Estévez-Braun A, Ravelo AG, Ferro EA, Tokuda H, Mukainaka T, *et al*. Inhibitory effects of lapachol derivatives on epstein-barr virus activation. Bioorg Med Chem 2003;11:483-8.

36. Park SH, Jeong SH, Kim SW. β-Lapachone Regulates the Transforming Growth Factor-β-Smad Signaling Pathway Associated with Collagen Biosynthesis in Human Dermal Fibroblasts. Biol Pharm Bull. 2016;39:524-31. doi: 10.1248/bpb.b15-00730.

37. Kim JH, Lee SM, Myung CH, Lee KR, Hyun SM, Lee JE, Park YS, Jeon SR, Park JI, Chang SE, Hwang JS. Melanogenesis inhibition of β-lapachone, a natural product from Tabebuia avellanedae, with effective in vivo lightening potency. Arch Dermatol Res. 2015, 307(3):229-38. doi: 10.1007/s00403-015-1543-5.

38. Souza-Silva F, do Nascimento SB, Bourguignon SC, Pereira BA, Carneiro PF, da Silva WS, *et al*. Evidences for leishmanicidal activity of the naphthoquinone derivative epoxy-α-lapachone. Exp Parasitol 2014;147:81-4.

39. Available from: https://www.rcsb.org/. [Last accessed on 2022 Jun 03].

40. Bissantz C, Folkers G, Rognan D. Protein-based virtual screening of chemical databases. 1.

41. Evaluation of different docking/scoring combinations. J Med Chem 2000;43:4759-67.

41. Trott O, Olson AJ. AutoDock Vina: Improving the speed and accuracy of docking with a new scoring function, efficient optimization, and multithreading. J Comput Chem 2010;31:455-61.

42. Jones G, Willett P, Glen RC. Molecular recognition of receptor sites using a genetic algorithm with a description of desolvation. J Mol Biol 1995;245:43-53.

43. Shaw DE Research. Schrödinger release 2020 3. Desmond molecular dynamics system. Maestro Desmond interoperability tools. Schrödinger: New York, NY, USA, 2020.

44. Patel HM, Ahmad I, Pawara R, Shaikh M, Surana S. *In silico* search of triple mutant T790M/C797S allosteric inhibitors to conquer acquired resistance problem in non-small cell lung cancer (NSCLC): A combined approach of structure-based virtual screening and molecular dynamics simulation. J Biomol Struct Dyn 2021;39:1491-505.

45. Ahmad I, Kumar D, Patel H. Computational investigation of phytochemicals from Withania somnifera (Indian ginseng/ashwagandha) as plausible inhibitors of GluN2B-containing NMDA receptors. J Biomol Struct Dyn. 2021;10:1-13. doi: 10.1080/07391102.2021.1905553.

46. Jorgensen WL, Maxwell DS, Tirado-Rives J. Development and testing of the OPLS all-atom force field on conformational energetics and properties of organic liquids. J Am Chem Soc 1996;118:11225-36.

47. Kalibaeva G, Ferrario M, Ciccotti G. Constant pressure-constant temperature molecular dynamics: A correct constrained NPT ensemble using the molecular virial. Mol Phys 2003;101:765-78.

48. Martyna GJ. Remarks on "Constant-temperature molecular dynamics with momentum conservation". Phys Rev E Stat Phys Plasmas Fluids Relat Interdiscip Topics 1994;50:3234-6.

49. Patel HM, Shaikh M, Ahmad I, Lokwani D, Surana SJ. BREED based de novo hybridization approach: Generating novel T790M/C797S-EGFR tyrosine kinase inhibitors to overcome the problem of mutation and resistance in non small cell lung cancer (NSCLC). J Biomol Struct Dyn 2021;39:2838-56.

50. Kadri A, Aouadi K. *in vitro* antimicrobial and α-glucosidase inhibitory potential of enantiopure cycloalkylglycine derivatives: Insights into their *in silico* pharmacokinetic, druglikeness, and medicinal chemistry properties. J App Pharm Sci 2020;10:107-15.

51. Othman IMM, Gad-Elkareem MAM, Hassane Anouar EH, Aouadi K, Kadri A, Snoussi M. Design, synthesis ADMET and molecular docking of new imidazo[4,5-b] pyridine-5-thione derivatives as potential tyrosyl-tRNA synthetase inhibitors. Bioorg Chem 2020;102:104105.

52. Ghannay S, Kadri A, Aouadi K. Synthesis, *in vitro* antimicrobial assessment, and computational investigation of pharmacokinetic and bioactivity properties of novel trifluoromethylated compounds using *in silico* ADME and toxicity prediction tools. Monatsh Chem 2020;151:267-80.

53. Alminderej F, Bakari S, Almundarij TI, Snoussi M, Aouadi K, Kadri A. Antioxidant activities of a new chemotype of *Piper cubeba* L. fruit essential oil (methyleugenol/eugenol): In silico molecular docking and ADMET studies. Plants (Basel) 2020;9:1534.

54. Zrieq R, Ahmad I, Snoussi M, Noumi E, Iriti M, Algahtani FD, *et al*. Tomatidine and patchouli alcohol as inhibitors of SARS-CoV-2 enzymes (3CLpro, PLpro and NSP15) by molecular docking and molecular dynamics simulations. Int J Mol Sci 2021;22:10693.

55. Ahmad I, Shaikh M, Surana S, Ghosh A, Patel H. p38α MAP kinase inhibitors to overcome EGFR tertiary C797S point mutation associated with osimertinib in non-small cell lung cancer (NSCLC): Emergence of fourth-generation EGFR inhibitor. J Biomol Struct Dyn 2022;40:3046-59.

56. Ayipo YO, Yahaya SN, Babamale HF, Ahmad I, Patel H, Mordi MN. β-Carboline alkaloids induce structural plasticity and inhibition of SARS-CoV-2 nsp3 macrodomain more potently than remdesivir metabolite GS-441524: Computational approach. Turk J Biol 2021;45:503-17.

57. Lee HY, Cho DY, Ahmad I, Patel HM, Kim MJ, Jung JG, *et al*. Mining of a novel esterase (est3S) gene from a cow rumen metagenomic library with organosphorus insecticides degrading capability: catalytic insights by site directed mutations, docking, and molecular dynamic simulations. Int J Biol Macromol 2021;190:441-55.

58. Pawara R, Ahmad I, Nayak D, Wagh S, Wadkar A, Ansari A, *et al*. Novel, selective acrylamide linked quinazolines for the treatment of double mutant EGFR-L858R/T790M non-small-cell lung cancer (NSCLC). Bioorg Chem 2021;115:105234.

59. Ahmad I, Jadhav H, Shinde Y, Jagtap V, Girase R, Patel H. Optimizing bedaquiline for cardiotoxicity by structure based virtual screening, DFT analysis and molecular dynamic simulation studies to identify selective MDR-TB inhibitors. *In silico* Pharmacol 2021;9:23.

60. Wu C, Liu Y, Yang Y, Zhang P, Zhong W, Wang Y, *et al*. Analysis of therapeutic targets for SARS-CoV-2 and discovery of potential drugs by computational methods. Acta Pharm Sin B 2020;10:766-88.

61. Bhuiyan FR, Howlader S, Raihan T, Hasan M. Plants metabolites: Possibility of natural therapeutics against the COVID-19 pandemic. Front Med (Lausanne) 2020;7:444.

62. Cheke RS. The molecular docking study of potential drug candidates showing anti-COVID-19 activity by exploring of therapeutic targets of SARS-CoV-2. EJMO 2020;4:185-95.

63. Prasansuklab A, Theerasri A, Rangsinth P, Sillapachaiyaporn C, Chuchawankul S, Tencomnao T. Anti-COVID-19 drug candidates: A review on potential biological activities of natural products in the management of new coronavirus infection. J Tradit Complement Med 2021;11:144-57.

64. Shoaib A, Azmi L, Shukla I, Alqahtani SS, Alsarra IA, Shakeel F. Properties of ethnomedicinal plants and their bioactive compounds: Possible use for COVID-19 prevention and treatment. Curr Pharm Des 2021;27:1579-87.

65. Chakravarti R, Singh R, Ghosh A, Dey D, Sharma P, Velayutham R, *et al.* A review on potential of natural products in the management of COVID-19. RSC Adv 2021;11:16711-35.

66. Adhikari B, Marasini BP, Rayamajhee B, Bhattarai BR, Lamichhane G, Khadayat K, *et al.* Potential roles of medicinal plants for the treatment of viral diseases focusing on COVID-19: A review. Phytother Res 2021;35:1298-312.

67. Ayatollahi SA, Sharifi-Rad J, Tsouh Fokou PV, Mahady GB, Ansar Rasul Suleria H, Krishna Kapuganti S, *et al.* Naturally occurring bioactives as antivirals: Emphasis on coronavirus infection. Front Pharmacol 2021;12:575877.

68. Alam MA, Parra-Saldivar R, Bilal M, Afroze CA, Ahmed MN, Iqbal HMN, *et al.* Algae-derived bioactive molecules for the potential treatment of SARS-CoV-2. Molecules 2021;26:2134.

69. Goc A, Sumera W, Rath M, Niedzwiecki A. Phenolic compounds disrupt spike-mediated receptor-binding and entry of SARS-CoV-2 pseudo-virions. PLoS One 2021;16:e0253489.

70. Biering SB, Van Dis E, Wehri E, Yamashiro LH, Nguyenla X, Dugast-Darzacq C, *et al.* Screening a library of FDA-approved and bioactive compounds for antiviral activity against SARS-CoV-2. ACS Infect Dis 2021;7:2337-51.

71. Maurya DK, Sharma D. Evaluation of traditional ayurvedic Kadha for prevention and management of the novel Coronavirus (SARS-CoV-2) using *in silico* approach. J Biomol Struct Dyn 2022;40:3949-64.